Arch. Metall. Mater. **64** (2019), 3, 925-930

DOI: 10.24425/amm.2019.129474

D. KONCZ-HORVÁTH*#, G. GERGELY*, Z. GYÖKÉR*, Z. GÁCSI*

RELIABILITY EXAMINATIONS OF SAC LEAD FREE SOLDER MATERIAL

In this paper the effect of soldering technique and thermal shock test were investigated on SAC 305 solder joints, produced by two different solder method. The solder joints were subjected to different cycle numbers up to 5000 thermal shock tests with two different thermal profiles of –30/+110°C and –40/+125°C. Microstructural properties of the tested joints were examined with the focus on intermetallic layer thickness and crack formation/propagation. Thickness of the scallop shaped Cu6Sn5 intermetallic layer was increased with increasing cycle number for both THRS and multiwave joints, but the thickening was more effective for the THRS joints. Cracks typically formed at the solder alloy/ PTH barrel and the solder alloy/pin interfaces and propagated along grain boundaries and precipitations of intermetallic compound.

Keywords: SAC, thermal shock test, intermetallic layer, crack

1. Introduction

The quality performance and long-term reliability of electrical parts, units, devices and equipment's are largely affected by operational conditions and service environment. For the reliability testing of solder interconnects used in commercial applications, reference test methods are specified by international standards and protocols. Thermal shock testing is performed to determine the ability of the tested product to consistently meet the criteria of safe and reliable operation upon exposure to thermal shock. During thermal shock tests thermo-mechanical loading conditions are created, thus accelerating early failure without reaching the upper temperature limit of the system.

Tanaka et al. [1] investigated tin-lead THT (through-hole) solder joints composed of a Pb-rich α phase and a Sn-rich β phase. The studied solder joints were subjected to high temperature storage tests, temperature cycle tests and thermal shock tests.

It was obvious from the High-Temperature Storage Test results, that the roughness of the α phase progressed with long-term exposure to heat. Inspecting the cross-section of the fracture surfaces, cracks were mostly found to propagate along the micro-cracked α phase. The mechanism of cracking was described as follows: a) thermal load promotes the coarsening of the α phase; b) under repeated thermal cycling, increasing stress is applied to the solder joints – due to differences in the thermal expansion coefficient of the component pin and the PCB; consequently, c) the α phase undergoes elongation stretching in the direction of stress, which enhances d) the occurrence of micro-cracks. Grain boundaries tend to roughen (in either phase) in response to stress, thus the joining strength of the Pb-Sn joint interface declines. This promotes e) crack propagation along the grain boundaries, followed by the micro-cracking and final degradation of the α phase. Upon thermal shock testing, fractures occurred at sites where the solder adjoined the lead pin or the Cu pad However, unlike in thermal cycling, no micro cracking of the α phase was observed. Heat stress caused by abrupt temperature change during thermal shock testing promoted the coarsening and peeling of the α phase in the intermetallic compound layer. Ding et al [2] studied the response of reflowed and wave soldered Sn-Pb solder joints to thermal fatigue testing (0 to 1200 cycles, –55°C to +125°C temperature range, 15 min dwell time). It was found that cracks in the reflow soldered joint propagated from solder surface to inner joint as a result of stress concentration deriving from the mismatch of various thermal expansion coefficients in the joint assembly. High stress rate due to thermal cycling occasionally caused PTH barrel fracturing and plastic solder joint deformation. As emphasized by the authors, the geometry of the solder joint played an important role in affecting solder joint reliability. In wave soldered joint specimens, the fillet shape notably influenced the stress releasing means, whereby some cracks got focused around the fillet surface (i.e. along the fillet lifting and at the corner of the plated copper layer (PCB)/ component pin) rather than in the inner solder. Considering intermetallic compound (IMC) formation, it was shown that the Cu6Sn5 intermetallic layer is considerably thicker in reflow soldered joints than in the wave soldered samples. Three typical crack initiation sites were identified. a) in the solder joint itself, due to plastic deformation caused by abrupt temperature change

* UNIVERSITY OF MISKOLC, FACULTY OF MATERIALS SCIENCE AND ENGINEERING, INSTITUTE OF PHYSICAL METALLURGY, METAL FORMING AND NANOTECHNOLOGY, HUNGARY

Corresponding author: femkhd@uni-miskolc.hu

during thermal fatigue testing; b) at the solder/PTH interface, resulting from CTE (coefficient of thermal expansion) mismatch; c) at the component pin/solder interface, which was attributed either to the poor solderability of the pin or the brittleness of Ni-Sn intermetallic layer (IML).

According to RoHS and WEEE regulations, Sn-Pb solder alloys were replaced with environmental friendly, Pb-free solder alloys. Similarly to Sn-Pb alloys, the most commonly used SAC (Sn-Ag-Cu) based alloys also suffer failure due to thermal loadings. The failure mechanisms of SAC solder joints have been discussed by several studies [3-6]. It was observed that failure develops with crack propagation in the bulk material in the vicinity of interfacial regions [7-9]. The results of thermo-mechanical fatigue testing (fatigue life tests, thermal shock tests) largely depend on the microstructure of the solder [10-13]. The mechanical properties of the bulk solder are obviously a function of as-solidified microstructure, yet the "destabilization" of this microstructure and the consequent recrystallization of the Sn phase due to thermal stress under thermal shock conditions pose considerable challenges to the reliability testing of solder joints [14]. Under the effect of high temperature during thermo-mechanical stress, high-density regions (i.e. regions of thermal stress concentration) undergo recrystallization, which leads to the nucleation and propagation of cracks along the recrystallized region. Recrystallization first evolves in strain concentrated areas then spreads through the bulk material, resulting in a crack profile representative of the heterogeneous microstructure [15-19].

Besides recrystallization, the thicked and brittle IML also plays an important role in failure of SAC solder joints. It was shown by Sadiq et al, that the thickness of the IMC within the bulk solder alloy increases with increasing isothermal aging time [20]. As for ball grid array (BGA) joints, it was observed in Ref. [21], that for the IMC growth during thermal shock is more notable than during thermal aging.

The aim of the present investigation is to follow the evolution of IML thickness and crack initiation/propagation during thermal shock tests of THT SAC solder joints produced by through hole reflow soldering and multiwave soldering. The microstructural characterization of SAC 305 is presented in our previous publication [22].

2. Experimental

Two sets of SAC 305 (provided by Henkel Ltd.) THT solder joints were produced. The first group was produced by through hole reflow soldering (THRS), while the other one was fabricated by multiwave soldering technique. Thermal cycling tests were carried out on the solder alloy with 30 min dwell time at temperature ranges of –30/+110°C and –40/+125°C, after 500; 1500; 3000, 4000 and 5000 thermal cycles. The thermal loading method was preferred over thermal aging (annealing), because thermal cycle tests are the most common in the electronic industry. Scanning electron microscopy (Zeiss EVO MA 10 SEM), energy dispersive spectrometry (EDS) and image analysis were used. Optical microscopy was carried out with a Zeiss Imager M1m microscope and AxioVision Rel. 4.8 software. Sections were prepared perpendicular to the length of the pins to measure the IML thickness. The examined section and the microstructure are shown in Fig. 1.

The sample preparation of test samples consisted of grinding, (320, 500, 800, 2000, 2400, 4000 SiC), polishing with 3 µm MD MOL + 1 µm diamond paste and etching with 93 ml metanol + 2 HCl + 3 ml HNO3. The IML thickness was measured by selecting the IML area and dividing it by the length of the selected area using image analysis. The method of IML thickness measurement is shown in Fig. 2.

3. Results and discussion

Fig. 3 shows series of micrographs of THRS and Multiwave solder joints subjected to thermal shock cycles with –30/+110°C thermal profile. Fig. 4. shows series of micrographs of THRS and multiwave solder joints subjected to thermal shock cycles with –40/+125°C thermal profile.

In Figs. 3-4 it can be seen that IMLs have scallop shape for both THRS and Multiwave techniques and both thermal profiles. The IMLs increase with increasing cycle number for both soldering techniques and thermal profiles. The top morphology (and shape) and the growth mechanism of IMCs were discussed by several researchers [23,24].

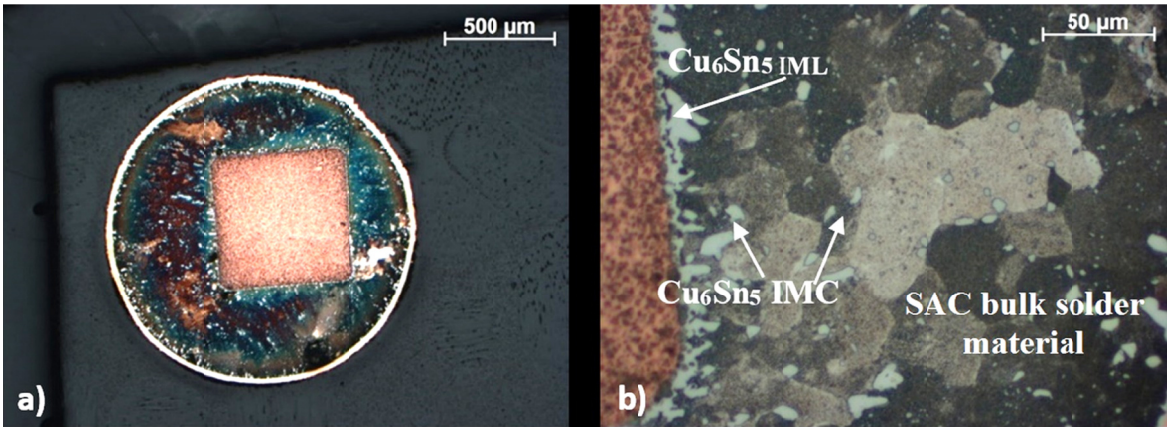

Fig. 1. a) Cross-section of the examined solder joint, b) microstructure of the solder joint

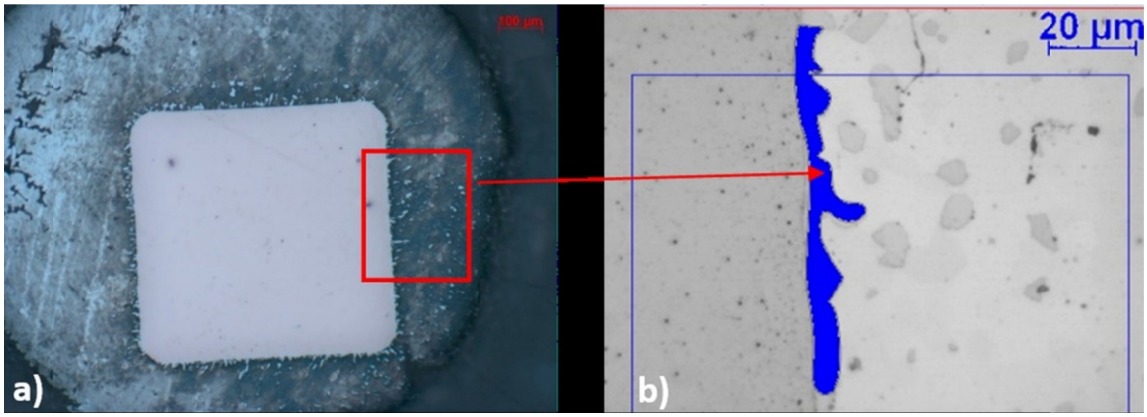

Fig. 2. a) Location of the IML thickness measurement of the examined solder joint, b) the IML thickness measurement method

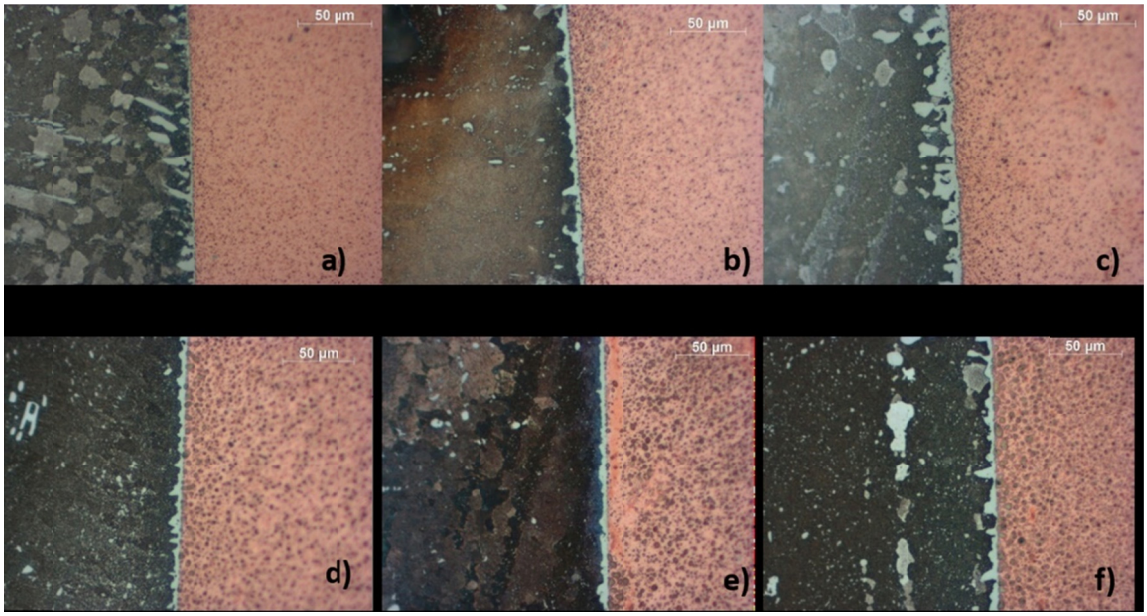

Fig. 3. a) Location of the IML thickness measurement of the examined solder joint, b) the IML thickness measurement method

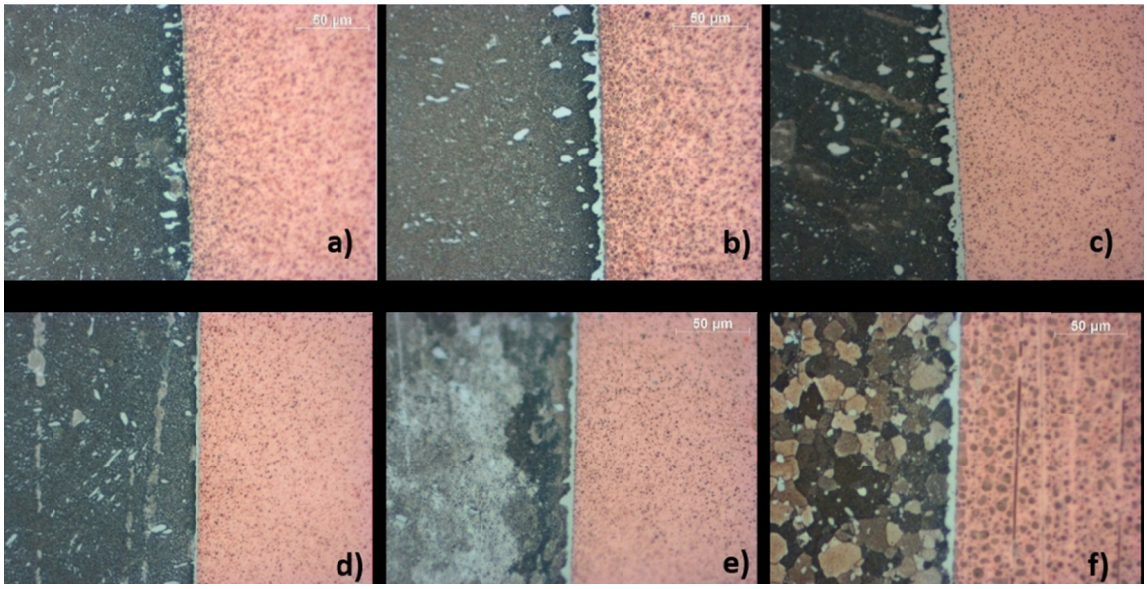

Fig. 4. Micrographs of the IML of samples subjected to thermal shock testing at –40/+125°C a) SAC 405 THRS, 500 cycles, b) SAC 405 THRS, 3000 cycles, c) SAC 405 THRS, 4000 cycles, d) SAC 305 multiwave, 500 cycles, e) SAC 305 multiwave, 3000 cycles, f) SAC 305 multiwave, 4000 cycles

Fig. 5 shows the obtained IML thickness values versus thermal cycle diagrams for both THRS and Multiwave samples and both thermal profiles. Initial IML thickness were 1.5 µm in –30/+110°C and 1.8 µm at –40/+125°C profile. Against to thermal cycle (5000TW) the values increased [25] and IML thickness was 8.1 (–30/+110°C) – 7.6 (–40/+125°C profile) µm in THRS samples. However, thermal cycle test resulted slightly increase of IML thickness in Multiwave sample, because initial values 1.3 (–30/+110°C) – 1.4 (–40/+125°C profile) were enhanced till 5.8 µm (–30/+110°C) and 5.5 µm (–40/+125°C profile). It can be concluded that interval of thermal profile has low effect, because IML thickness values were near the same in both alloys. In low TW situation, IML thickness changed simultaneously in both alloys, however in case of 3000, 4000 and 5000 TW, the growth of IML layer was more severe in THRS samples that is IML thickness grow was more pronounced for the THRS samples than for the Multiwave samples. Multiwave soldering resulted lower IML thickness due its higher process speed [26], thus, the number of Cu6Sn5 intermetallic compounds (IMC) are much higher in Multiwave samples than in THRS samples. It can be the reason that IML in Multiwave samples had slight grow than in THRS samples in high TW situations.

Crack length versus cycle number is presented in Fig. 6. Interval of thermal profile had no significant effect of crack length in any samples, that is app. same crack length were measured in both type of samples at same TW independently from the interval of thermal profile. In case of both thermal profile high TW resulted more than two times higher crack length in Multiwave samples than in THRS samples.

The explanation of this phenomena is due to the different soldering technology and is related to the thickness of the layer. Lower IML was measured in Multiwave samples (app. half) than in THRS samples (Fig. 5.) in high TW situation. Thus, the number of Cu6Sn5 intermetallic compounds (IMC) are much higher in Multiwave samples than in THRS samples. Due to thermal cycles IMCs coarsen and larger numbers of coarsened grains result larger cracks.

Fig. 7 shows SEM images of the Multiwave sample subjected to 500 cycles of –40/+125°C thermal profile. The crack formed in the solder fillet and propagated along precipitation of the Cu6Sn5 phase (point 1). SEM images of the THRS sample in case of 500 cycles of –40/+125°C thermal profile are represented by Fig. 8. The crack formed at the pin/solder alloy interface and propagated along the Cu6Sn5 phase (point 1).

SEM images demonstrate that soldering defects – located primarily at the component pin/solder or solder/PTH barrel interface – are the most common initiation sites for fatigue crack propagation towards the inside of the solder joint. Propagation paths follow primarily the boundaries of intermetallic compound phases.

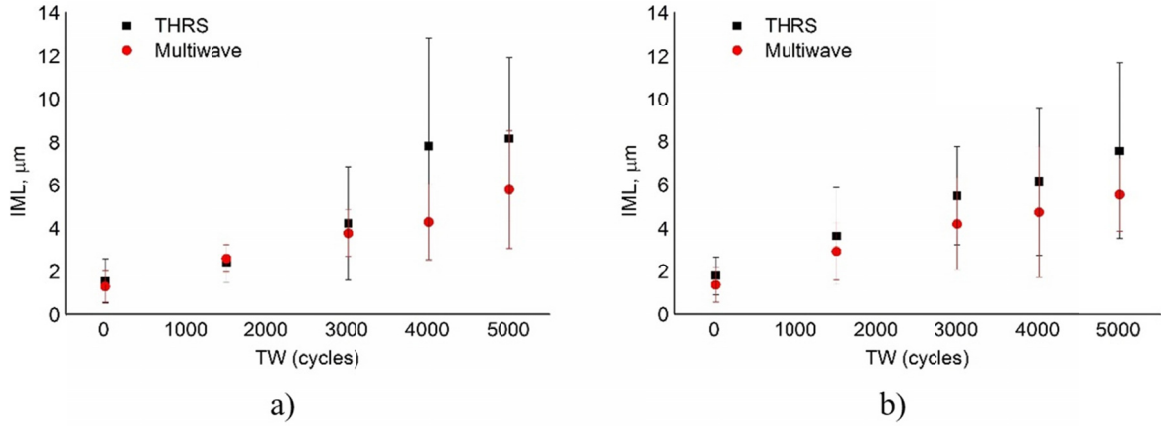

Fig. 5. IML thickness versus cycle number a) –30/+110°C thermal profile, b) –40/+125°C thermal profile

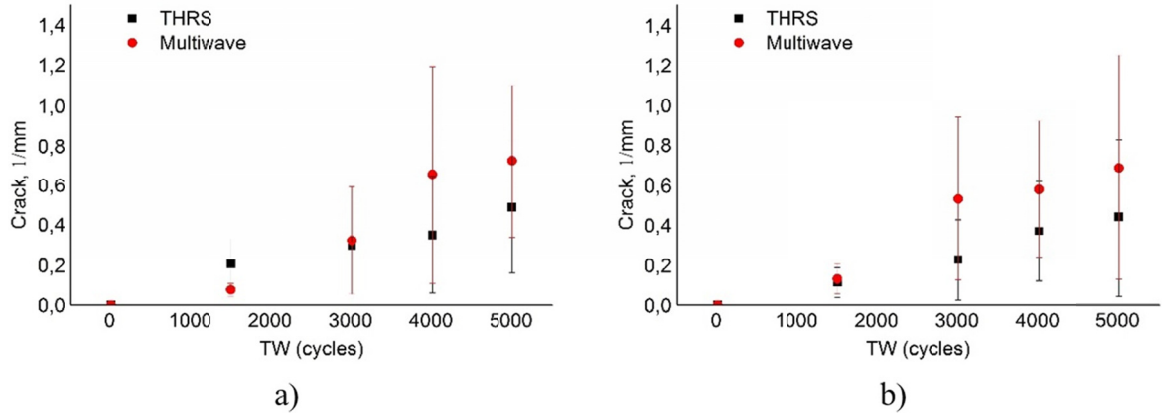

Fig. 6. Crack length versus cycle number a) –30/+110°C thermal profile, b) –40/+125°C thermal profile

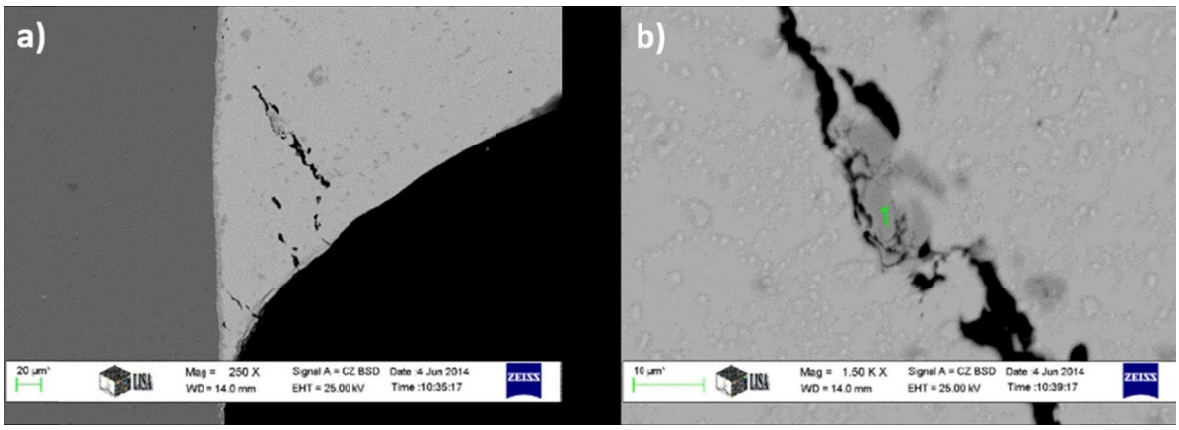

Fig. 7. SEM micrographs of the SAC 305 multiwave sample subjected to 500 cycles of thermal shock with –40/+125°C thermal profile a) crack in the fillet, b) the crack with higher magnification

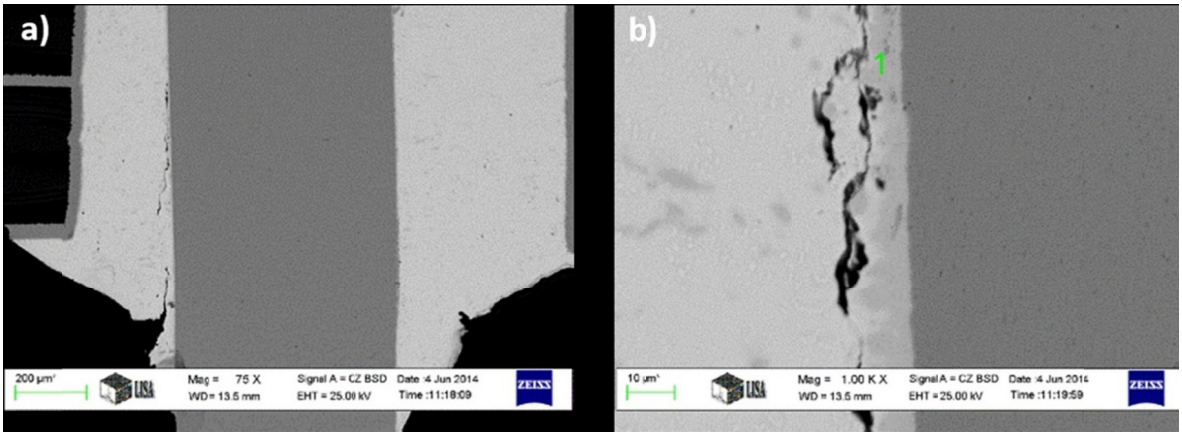

Fig. 8. SEM micrographs of SAC 405 THRS sample subjected to 500 cycles of thermal shock with –40/+125°C thermal profile a) crack near the pin/solder alloy interface, b) the crack with higher magnification

4. Conclusions

SAC solder joints produced by Multiwave and THRS soldering technique were subjected to different interval thermal shock tests. In this paper the effect of production method and thermal profile were experimentally studied on the microstructure.

a. The IML, formed at the pin/solder alloy interface, got thick with increasing thermal shock cycle in both type of joints. This phenomena was more pronounced in joints produced by THRS technique than that of in multiwave soldered joints. The thinner Cu6Sn5 thickness in multiwave joint is probably due to the different process time of techniques, i.e. less process time result thin IML layer and of course higher number of IMCs.
b. Multiwave sample had two times higher crack length than in THRS samples, because the roughening of higher number of IMCs resulted higher crack length.
c. Two typical crack initiation sites were identified in the samples. Cracks were located at the solder/PTH barrel interface in Multiwave samples – supposedly due to CTE (coefficient of thermal expansion) mismatch; while in case of THRS samples cracks formed at the component pin/solder interface probably deriving from soldering defects (void formation, pin hole, defective pin insertion, poor hole fill). Crack propagation paths were either directed from solder surface to the inner joint or proceeded intergranularly along Sn grain boundaries parallel to the solder joint, without penetrating the IMC phases.
d. Applied thermal profile had no significant effect nor at IML thickness and neither at crack length.

Acknowledgments

The described article was carried out as part of the GINOP-2.3.2-15-2016-00027 "Sustainable operation of the workshop of excellence for the research and development of crystalline and amorphous nanostructured materials" project implemented in the framework of the Szechenyi 2020 program. The realization of this project is supported by the European Union.

REFERENCES

[1] H. Tanaka, Y. Aoki, S. Yamamoto, ESPEC Technology Report 3, 25-29 (1997).

[2] Y. Ding, C.Q. Wang, Y.H. Tian, ICEPT2003 Proc.
[3] D.R. Frear, L.N. Ramanathan, J-W. Jang, N.L. Owens, Proc. 46th IEEE, 450-454 (2008).
[4] P. Lauro, S.K. Kang, W.K. Choi, D.Y. Shih, J. of Elect. Mat., 1432-1440 (2003).
[5] S. Terashima, T. Kobayashi, M. Tanaka, Sci. Technol. Weld. Join. 732-738 (2008).
[6] T.T. Mattila, M. Mueller, M. Paulasto-Krockel, K-J. Wolter, Proc. 3rd IEEE-ESTC,1-8 (2010).
[7] F.A. Stam, E. Davitt, Microel. Reliab. **41**, 1815-1822 (2001).
[8] M.N. Collins, E. Dalton, J. Punch, J. of Alloys and Comp. **688**, 164-170 (2016).
[9] X. Hui, L. Xiaoyan, Y. Yongchang, L. Na, S. Yaowu, Rare Met. Mat. and Eng. **42**, 2, February (2013).
[10] Y. Ding, R. Tian, X. Wang C. Hang, F. Yua, L. Zhou, X. Meng, Y. Tian, Microel. Reliab. **55**, 2396-2402 (2015).
[11] J.W.C. de Vries, M.Y. Jansen, W.D. van Driel, Microel. Reliab. **47**, 444-449 (2007).
[12] D.A. Shnawah, M.F.M. Sabri, I.A. Badruddin, Microel. Reliab. **52**, 90-99 (2012).
[13] J.J. Sundelina, S.T. Nurmi, T.K. Lepisto, E.O. Ristolainen, Mat. Sci. and Eng. A **420,** 55-62 (2006).
[14] L. Snugovsky, P. Snugovsky, P.P. Perovic, J.W. Rutter, Mat. Sci. and Tech. **21**, 1, 61-68 (2005).
[15] T. Laurila, T. Mattila, V. Vuorinen, J. Karppinen, J. Lia, M. Sippola, J.K. Kivilahti, Microel. Reliab. **47**, 1135-1144 (2007).
[16] J. Han, F. Guo, J.P. Liu, J. of Alloys and Comp. **704**, 574-584 (2017).
[17] J. Han, F. Guo, J.P. Liu, J. of Alloys and Comp. **698**, 706-713 (2017).
[18] J. Li, H. Xu, T.T. Mattila, J.K. Kivilahti, T. Laurila, M. Paulasto-Kröckel, Comp. Mat. Sci. **50**, 690-697 (2010).
[19] J.J. Sundelina, S.T. Nurmi, T.K. Lepisto, Mat. Sci. and Eng. A **474**, 201-207, (2008).
[20] M. Sadiq, R. Pesci, M. Cherkaoui, J. of Elect. Mat. **42**, 3 (2013).
[21] Y. Tian, X. Liu, J. Chow, Y.P. Wu, S.K. Sitaraman, J. of Elect. Mat. **42**, 8 (2013).
[22] A. Molnar, D. Janovszky, I. Kardos, I. Molnar, Z. Gacsi, J. of Elect. Mat. **44**, 10 (2015).
[23] X. Yanghua, X. Xiaoming, L. Chuanyan, J. of Mat. Sci. **41**, 8, 2359-2364 (2006).
[24] C. Guohai, L. Xiaoyan, M. Jusheng, J. of Elect. Mat. **35**, 10 (2006).
[25] D. Shangguan, Lead-Free Solder Interconnect Reliability, ASM International, (2005).
[26] M. Schaefer, W.Laub, J.M.Sabee, R.A.Fournelle, P.S.Lee, J. of Elect. Mat. **25**, 6, pp 992-1003 **(**1996).